Prediction of Individual Brain Maturity Using fMRI

Nico U. F. Dosenbach, *et al.*

Science **329**, 1358 (2010);
DOI: 10.1126/science.1194144

CORRECTED 5 NOVEMBER 2010; SEE LAST PAGE

activity (Fig. 3B). Mutation of Phe155 to alanine severely impaired crRNA processing, suggesting that this residue also plays an important role in substrate orientation. However, none of the above mutations severely disrupted crRNA binding, as judged by means of electrophoretic mobility shift assays, indicating that the structural integrity of the mutant proteins was not compromised (fig. S8). Thus, interaction between Csy4 and the closing base pair of the RNA stem is critical for pre-crRNA processing, whereas sequence-specific recognition of the penultimate base pair in the stem is less important. Incubation of Csy4 with a panel of short RNA oligonucleotides containing a variety of mutations in the CRISPR repeat stem-loop sequence further confirmed that Csy4 requires a C-G base pair closing the RNA stem and that Csy4 can accommodate different nucleotides at the penultimate RNA base pair (fig. S10).

Phylogenetic analysis of CRISPR loci suggests that CRISPR repeat sequences and structures have co-evolved with the Cas genes (*19*). The similarity of Csy4 at the fold level to the CRISPR-processing endonucleases CasE and Cas6 suggests that collectively they are likely to have descended from a single ancestral endoribonuclease enzyme that has diverged throughout evolution. The structure described here reveals how Csy4 and related endonucleases from the same CRISPR/Cas subfamily use an exquisite recognition mechanism to discriminate crRNA substrates from other cellular RNAs. This illustrates the importance of co-evolution in shaping molecular recognition mechanisms in the CRISPR pathway. Furthermore, the ability of Csy4 to form a tight complex with the cleaved crRNA product points to Csy4 having a functional role within the CRISPR pathway that extends beyond pre-crRNA cleavage.

References and Notes

1. S. J. Brouns *et al.*, *Science* **321**, 960 (2008).
2. J. Carte, R. Wang, H. Li, R. M. Terns, M. P. Terns, *Genes Dev.* **22**, 3489 (2008).
3. D. H. Haft, J. Selengut, E. F. Mongodin, K. E. Nelson, *PLOS Comput. Biol.* **1**, e60 (2005).
4. C. R. Hale *et al.*, *Cell* **139**, 945 (2009).
5. K. S. Makarova, N. V. Grishin, S. A. Shabalina, Y. I. Wolf, E. V. Koonin, *Biol. Direct* **1**, 7 (2001).
6. R. Barrangou *et al.*, *Science* **315**, 1709 (2007).
7. L. A. Marraffini, E. J. Sontheimer, *Science* **322**, 1843 (2008).
8. L. A. Marraffini, E. J. Sontheimer, *Nat. Rev. Genet.* **11**, 181 (2010).
9. J. van der Oost, M. M. Jore, E. R. Westra, M. Lundgren, S. J. Brouns, *Trends Biochem. Sci.* **38**, 401 (2009).
10. R. Jansen, J. D. Embden, W. Gaastra, L. M. Schouls, *Mol. Microbiol.* **43**, 1565 (2002).
11. I. Grissa, G. Vergnaud, C. Pourcel, *BMC Bioinformat.* **8**, 172 (2007).
12. T. H. Tang *et al.*, *Proc. Natl. Acad. Sci. U.S.A.* **99**, 7536 (2002).
13. R. K. Lillestøl, P. Redder, R. A. Garrett, K. Brügger, *Archaea* **2**, 59 (2006).
14. R. K. Lillestøl *et al.*, *Mol. Microbiol.* **72**, 259 (2009).
15. T. H. Tang *et al.*, *Mol. Microbiol.* **55**, 469 (2005).
16. Materials and methods are available as supporting material on *Science* Online.
17. A. Ebihara *et al.*, *Protein Sci.* **15**, 1494 (2006).
18. L. Holm, C. Sander, *J. Mol. Biol.* **233**, 123 (1993).
19. V. Kunin, R. Sorek, P. Hugenholtz, *Genome Biol.* **8**, R61 (2007).
20. P. Legault, J. Li, J. Mogridge, L. E. Kay, J. Greenblatt, *Cell* **93**, 289 (1998).
21. A. Huppler, L. J. Nikstad, A. M. Allmann, D. A. Brow, S. E. Butcher, *Nat. Struct. Biol.* **9**, 431 (2002).
22. Z. Cai *et al.*, *Nat. Struct. Biol.* **5**, 203 (1998).
23. X. Ye, A. Gorin, A. D. Ellington, D. J. Patel, *Nat. Struct. Biol.* **3**, 1026 (1996).
24. K. Anand, A. Schulte, K. Vogel-Bachmayr, K. Scheffzek, M. Geyer, *Nat. Struct. Mol. Biol.* **15**, 1287 (2008).

25. We thank W. Westphal for help with purification of Csy4 constructs; J. van der Oost for discussion; J. Doudna Cate and members of the Doudna laboratory for critical reading of the manuscript; and C. Ralston and J. Holton (Beamlines 8.2.2 and 8.3.1, Advanced Light Source, Lawrence Berkeley National Laboratory) and S. Coyle for assistance with X-ray data collection. R.E.H. is supported by the U.S. NIH training grant 5 T32 GM08295. M.J. is supported by a Human Frontier Science Program Long-Term Fellowship. B.W. is a Howard Hughes Medical Institute Fellow of the Life Sciences Research Foundation. This work was supported in part by grants from NSF and the Bill and Melinda Gates Foundation. J.A.D. is a Howard Hughes Medical Institute Investigator. Coordinates and structure factors for the Csy4-crRNA complex have been deposited in the Protein Data Bank under accession codes 2xli, 2xlj, and 2xlk. The authors have filed a related patent.

Supporting Online Material

www.sciencemag.org/cgi/content/full/329/5997/1355/DC1
Materials and Methods
Figs. S1 to S10
Table S1
References

13 May 2010; accepted 22 July 2010
10.1126/science.1192272

Prediction of Individual Brain Maturity Using fMRI

Nico U. F. Dosenbach,[1]* Binyam Nardos,[1] Alexander L. Cohen,[1] Damien A. Fair,[2] Jonathan D. Power,[1] Jessica A. Church,[1] Steven M. Nelson,[1,3] Gagan S. Wig,[1,4,5] Alecia C. Vogel,[1] Christina N. Lessov-Schlaggar,[6] Kelly Anne Barnes,[1] Joseph W. Dubis,[1] Eric Feczko,[6] Rebecca S. Coalson,[1,7] John R. Pruett Jr.,[6] Deanna M. Barch,[3,6,7] Steven E. Petersen,[1,3,7,8] Bradley L. Schlaggar[1,7,8,9]*

Group functional connectivity magnetic resonance imaging (fcMRI) studies have documented reliable changes in human functional brain maturity over development. Here we show that support vector machine-based multivariate pattern analysis extracts sufficient information from fcMRI data to make accurate predictions about individuals' brain maturity across development. The use of only 5 minutes of resting-state fcMRI data from 238 scans of typically developing volunteers (ages 7 to 30 years) allowed prediction of individual brain maturity as a functional connectivity maturation index. The resultant functional maturation curve accounted for 55% of the sample variance and followed a nonlinear asymptotic growth curve shape. The greatest relative contribution to predicting individual brain maturity was made by the weakening of short-range functional connections between the adult brain's major functional networks.

Functional magnetic resonance imaging (fMRI) holds the promise that it may one day aid in the diagnosis of developmental delays and neuropsychiatric disorders, especially for conditions that lack structural brain abnormalities. Much progress has been made describing typical and atypical human brain activity at the group level with use of fMRI. However, determining whether single fMRI scans contain sufficient information to classify and make predictions about individuals remains a critical challenge (*1*).

The work described here had two major objectives. The first aim was to develop an approach for making accurate predictions about individuals on the basis of single fMRI scans. The second aim, building on the first, was to further illuminate typical brain development, a prerequisite for studying developmental disorders and pediatric-onset neuropsychiatric diseases (*2*, *3*).

Previous developmental fMRI studies have shown reliable differences between children and adults (*4*–*9*). Thus, we set out to push the study of functional brain maturation toward making predictions about single individuals. We used multivariate pattern analysis (MVPA) tools (*10*–*14*) to make continuously valued predictions about the relative functional maturity levels of individual brains.

[1]Department of Neurology, Washington University School of Medicine, St. Louis, MO 63110, USA. [2]Department of Psychiatry, Oregon Health and Science University, Portland, OR 97239, USA. [3]Department of Psychology, Washington University, St. Louis, MO 63130, USA. [4]Department of Psychology, Harvard University, Cambridge, MA 02138, USA. [5]Athinoula A. Martinos Center for Biomedical Imaging, Massachusetts General Hospital, Charlestown, MA 02129, USA. [6]Department of Psychiatry, Washington University School of Medicine, St. Louis, MO 63110, USA. [7]Department of Radiology, Washington University School of Medicine, St. Louis, MO 63110, USA. [8]Department of Anatomy and Neurobiology, Washington University School of Medicine, St. Louis, MO 63110, USA. [9]Department of Pediatrics, Washington University School of Medicine, St. Louis, MO 63110, USA.

*To whom correspondence should be addressed. E-mail: ndosenbach@wustl.edu (N.U.F.D.); schlaggarb@neuro.wustl.edu (B.L.S.)

MVPA applies sophisticated machine-learning algorithms (*12*, *14*) to the complex patterns generated by a myriad of measurements, termed features. We chose support vector machines (SVMs) as our classification and prediction algorithms because they are resilient to overfitting and allow the extraction of feature weights (*15*, *16*). Because of its sensitivity, MVPA has become increasingly used in task-evoked neuroimaging, beginning with early work by Haxby and colleagues (*10*). When applied to task-related fMRI data, MVPA has allowed researchers to accomplish impressive feats, such as extracting patterns related to memory reinstatement (*17*), predicting which nouns participants heard (*18*), and exploring the neural correlates of consciousness (*19*, *20*).

However, in many pediatric and clinical populations, the acquisition of task-related data becomes increasingly difficult because of a variety of causes (e.g., ability to perform task). Therefore, we used functional connectivity MRI (fcMRI) data, which can be collected quickly and easily under different conditions, including but not limited to anesthesia, sleep, and quiet rest (*21*). Resting-state fcMRI (rs-fcMRI) studies measure the correlations in spontaneous activity between brain regions (*22*). These rs-fcMRI measurements are reliable across scans and institutions (*23*) and are thought to have been shaped by the cumulative effect of experiences across one's lifespan (*24*).

Thus, we developed a functional connectivity MVPA (fcMVPA) approach that combines the sensitivity of MVPA with the robust and easy data acquisition of fcMRI. To build a machine that could predict the functional maturity level of individual brains from about 5 min of fMRI data, we used 238 rs-fcMRI scans (3 T; continuous rest) from typically developing participants ranging in age from 7 to 30 years (tables S1 and S2). Blood oxygen level–dependent (BOLD) time courses were generated for 160 regions of interest (ROIs) derived from a series of meta-analyses of task-related fMRI studies that cover much of the brain (fig. S1 and table S3). All possible interregional temporal correlations, or functional connections (n = 12,720), were computed for each individual. By using standard MVPA methodology to avoid circularity bias (*14*), we first reduced the number of features to the 200 functional connections most reliably different between children and adults in each round of leave-one-out cross-validation (*16*).

Binary SVM classification of individuals as either children (61 scans of 7- to 11-year-olds; mean = 9.4) or adults (61 scans of 24- to 30-year-olds; mean = 26.2), matched for brain volume and in-scanner movement, was 91% accurate (permutation test, $P < 0.0001$; 90% sensitive; 92% specific).

To assess the relative functional brain maturity of individuals more precisely, we used SVM regression (SVR). Chronological age served as the training measure for SVR brain maturity prediction because, in contrast to other potential measures of maturity such as hormone levels or developmental milestones, age is easily obtained and free of measurement error. In this manner, we generated a predicted "brain age" as an estimate of each participants' functional maturity level. Achieving functional brain maturity in this sense is likely the consequence of integrated processes that are both developmental (e.g., myelination and synaptic pruning) and experiential.

The predicted brain ages for all scans were converted to a functional connectivity maturation index (fcMI) by setting the mean predicted brain age of typically developed young adults (18 to 30 years old) equal to 1.0. The fcMI thus represents a 200-dimensional, weighted index of an individual's overall functional brain maturity.

Model selection analyses were carried out by using Akaike information criterion (AIC) weights (*16*, *25*). These analyses showed that functional maturity levels between the ages of 7 and 30 years, as measured by fcMI, are best fit by classic biological models of asymptotic growth or maturation (*26*), such as Von Bertalanffy's growth curve or the Pearl-Reed logistic growth curve (Fig. 1 and table S4).

The most probable models of functional brain maturation provided almost identical curve fits in the 7- to 30-years-old age range (Fig. 1 and fig. S2). Linear models generated the poorest fits (fig. S2 and table S4). The best fitting models showed asymptotic maturation toward a predicted population mean maximum brain age of ~22 years, corresponding to an fcMI of slightly greater than 1.0. The fitted models mainly differed in their predictions for younger ages. The two-parameter Von Bertalanffy curve predicts more rapid maturation between birth and age 7 years than the three-parameter Pearl-Reed curve. Future collection of additional rs-fcMRI scans between birth and age 7 years should help decide between these interesting alternatives.

For independent replication, the same analyses were also carried out on two other large-scale developmental functional connectivity data sets with somewhat different characteristics. Data set 2 consisted of 195 fcMRI scans (age 7 to 31 years; 1.5 T) where rest periods had been extracted from blocked fMRI designs. Data set 3 consisted of 186 event-related fMRI scans (age 6 to 35 years) that were made more similar to resting state by regressing out task effects. Despite these differences in the type of functional connectivity data, binary adult-versus-child classification results replicated (accuracy of 92% for data set 2 and 93% data set 3), as did the functional brain maturity prediction results (data set 2, $r^2 = 0.519$; data set 3, $r^2 = 0.557$) (figs. S3 and S4, and table S4). After separately generating fcMI values for each data set, 613 scans between the ages of 6 and 30 years were combined into a single, "mixed-type" functional connectivity maturation curve (figs. S5 and S6), with very similar properties to the pure 3-T rs-fcMRI maturation curve (Fig. 1). Six participants older than 30 years from data sets 2 and 3 were excluded from the fits for consistency across data sets. These findings demonstrate that fcMRI-based maturation analyses generalize across cohorts and different types of fcMRI data.

A crucial aspect of MVPA is displaying and analyzing the features that drive the multivariate predictor. Therefore, we extracted the weighting assigned to each feature (i.e., functional connection) by the predictor and displayed the 156 consensus features (*16*) from the SVR maturity prediction (data set 1) scaled by their weights (Fig. 2 and fig. S7). The resulting pattern of feature weights verified and expanded on findings from prior developmental rs-fcMRI studies (*7*, *8*, *27*). These previous studies, which were based on smaller sets of regions and sample numbers, had suggested that the brain's functional organization is dominated by more local

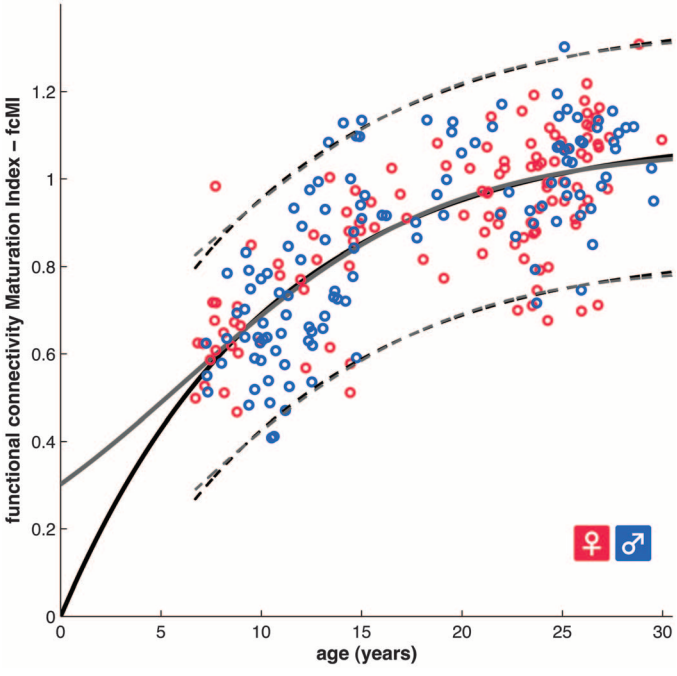

Fig. 1. Functional brain maturation curve. Individual functional brain maturity levels of 238 rs-fcMRI scans (115 females) between the ages of 7 to 30 years. Chronological age is shown on the x axis and the fcMI on the y axis (females pink, males blue). The fit for the Von Bertalanffy's equation [$a \bullet (1 - e^{-bx})$, $r^2 = 0.553$, permutation test, $P < 0.001$, AIC weight = 0.3] is shown with a solid black line. The fit for the Pearl-Reed equation [$a/(1 + b \bullet e^{-cx})$, $r^2 = 0.555$, AIC weight = 0.23] is shown with a solid gray line. The 95% prediction limits are shown with dashed lines.

interactions between brain regions in children and shifts to a more distributed architecture in young adults.

The fcMVPA brain maturity predictor has its basis in two types of functional connections, those whose strengths were positively correlated (strengthening) with chronological age and those that were negatively correlated (weakening) with chronological age (Fig. 2, figs. S7 and S8, and table S5). As previously noted (*7*, *8*, *27*), functional connections that grew in strength across development were significantly longer (mean = 80 mm) than functional connections that diminished in strength (37 mm) [$t(154) = 14.66$, $P < 1 \times 10^{-30}$] (figs. S7 and S8). In addition, we found that functional connections increasing in strength were significantly more likely to run along the anterior-posterior (AP) axis in the horizontal plane (mean angle = 37°) than the functional connections that became weaker (58°) [$t(154) = 4.84$, $P < 1 \times 10^{-5}$]. The quantitative nature of the MVPA approach also allowed us to extract the relative contributions of weakening and strengthening functional connections. These analyses revealed that weakening connections contributed more to predicting brain maturity (68%) than strengthening connections (32%), a finding better visualized by separately summing weights for both weakening and strengthening features (Fig. 3).

To extract the relative contributions of different ROIs to maturity prediction, we computed their node or ROI weights by summing the weights across all functional connections for each ROI (Fig. 2, fig. S9, and table S6).

Some of the regions in ventromedial prefrontal cortex and parietal cortex have previously been associated with the brain's default-mode network (*28*), whereas other anterior, dorsolateral, and medial prefrontal regions are known to be important for cognitive control (*4*, *6*, *29*). Hence, we assessed the network affiliations of each ROI more formally by performing modularity optimization on the average adult functional connectivity matrix (*8*). Doing so partitioned the 160 ROIs into six networks: cingulo-opercular, frontoparietal, default mode, sensorimotor, occipital, and cerebellar (Figs. 2 and 3 and fig. S9) (*8*, *30*).

Separately summing the feature weights for each network (Fig. 3) revealed that the cingulo-opercular control network had the greatest sum total of feature weights, meaning that it was the relatively best predictor, but all six identified networks made sizeable contributions toward predicting functional maturity. Separating functional connection weights according to whether the connections occur within or between networks (Fig. 3) revealed that the vast majority of predictor weights for within-network connections were assigned to strengthening connections (Fig. 3, left). In contrast, most of the weights for between-network connections were taken up by connections that weaken (Fig. 3, right). This pattern is consistent with the internal strengthening of the adult brains' six identified major functional networks, as well as the sharpening of the boundaries between them.

The region with the greatest relative prediction power about brain maturity was the right anterior prefrontal cortex [Montreal Neurological Institute (MNI): 27, 49, 26], thought to be important for cognitive control and higher-order

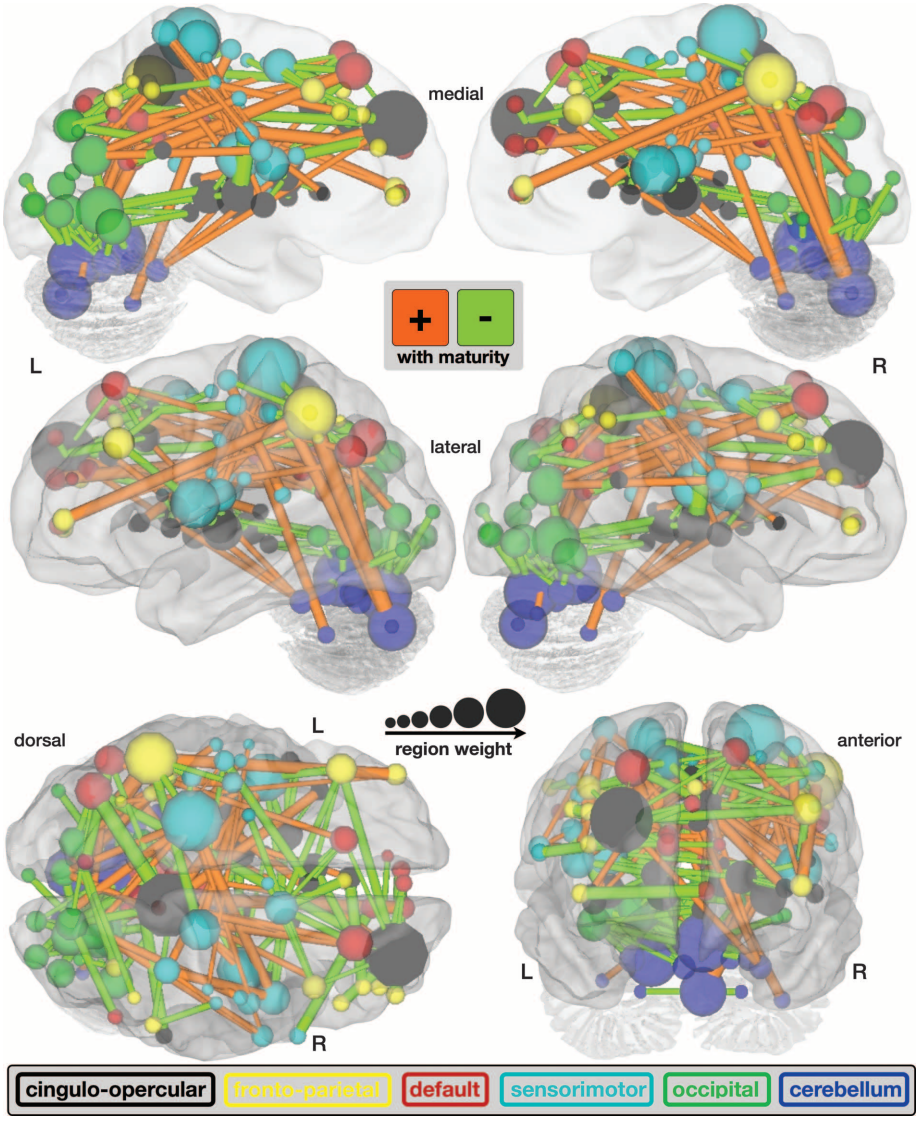

Fig. 2. fcMVPA connection and region weights. The functional connections driving the SVR brain maturity predictor are displayed on a surface rendering of the brain. The thicknesses of the 156 consensus functional connections scale with their weights. Connections positively correlated with age are shown in orange, whereas connections negatively correlated with age are shown in light green. Also displayed are the 160 ROIs scaled by their weights (1/2 sum of the weights of all the connections to and from that ROI). The ROIs are color-coded according to the adult rs-fcMRI networks (cingulo-opercular, black; frontoparietal, yellow; default, red; sensorimotor, cyan; occipital, green; and cerebellum, dark blue).

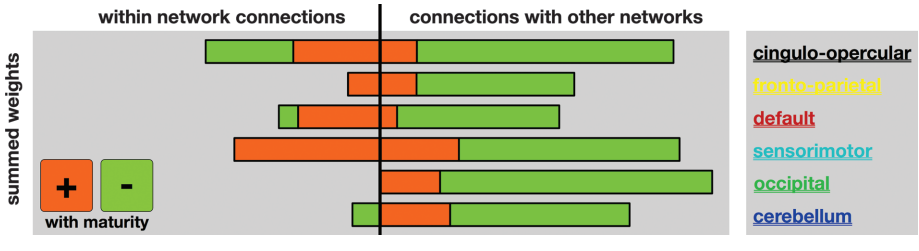

Fig. 3. SVR brain maturity weights by adult rs-fcMRI networks. The sums of all the functional connection weights within each network are shown to the left of the vertical black line. The sums of all the functional connection weights between networks are shown to the right.

reasoning (*4*, *6*, *9*, *29*). The precuneus, which has recently been found to be the most highly structurally (*31*) and functionally (*32*) connected brain region, contained the second most predictive ROI (MNI: 8, –40, 50). It stands to reason that regions such as those in the precuneus, situated at the center of the adult brain's connectome, could carry much information about how the network develops.

The results presented here strongly suggest that the fcMVPA approach derives its accuracy from important neurophysiologic changes. The functional connectivity maturation curve (Fig. 1 and fig. S6) has a biologically plausible asymptotic shape, first used to describe the growth of animals (Von Bertalanffy) and human populations in the setting of limited resources (Pearl-Reed) (*26*). Similarly shaped growth curves that plot measures such as height and head circumference against age are used routinely in pediatric medicine. The maturation curves suggest that mean population functional brain maturity asymptotes toward a maturity level or brain age of ~22 years (*33*). The shape of the functional maturation curve highlights the nonlinear nature of functional brain maturation (*34*, *35*).

The pattern of fcMVPA feature weights indicated that functional maturation is driven both by the segregation of nearby functional areas, through the weakening of short-range functional connections, and the integration of distant regions into functional networks, by strengthening of long-range functional connections (fig. S7) (*2*, *7*, *8*, *27*). It is interesting that fcMVPA revealed the relatively greater importance of functional segregation when compared to functional integration for the prediction of functional brain maturity. In addition, fcMVPA showed that functional integration is mainly carried by longer-range functional connections along the AP axis. Grouping brain regions into functional networks (*8*) showed that both integration within functional networks and segregation between them are widely distributed across the cortex and cerebellum.

Several important, large-scale structural MRI studies of brain maturation have already mapped out anatomical maturation curves for a variety of measures (*33*, *34*, *36*, *37*). The present study provides a functional counterpart to the prior anatomical studies. In addition, it combines the most relevant features into a single index instead of separately listing different measures. It should be informative to apply similar MVPA methods to the study of structural brain maturation, as well as combining MVPA of structural and functional data.

Important group-level rs-fcMRI studies have already shown differences in spontaneous activity in disorders such as autism, schizophrenia, depression, and attention-deficit hyperactivity disorder (*21*). Hence, imaging-based binary classification studies of clinical populations are starting to be pursued (*38*). The use of SVR in fcMVPA to make continuously valued predictions may become relevant in clinical scenarios where binary classification is insufficient (e.g., to predict years until Alzheimer's disease symptom onset).

The standard clinical workup for many developmental neuropsychiatric disorders already includes a structural MRI scan of the brain. The present observations suggest that the addition, at little extra cost, of a brief resting acquisition to the standard clinical study could one day provide useful information to aid in the screening, diagnosis, and prognosis of individuals with disordered brain function.

References and Notes

1. R. A. Poldrack, Y. O. Halchenko, S. J. Hanson, *Psychol. Sci.* **20**, 1364 (2009).
2. M. H. Johnson, *Nat. Rev. Neurosci.* **2**, 475 (2001).
3. T. Paus, M. Keshavan, J. N. Giedd, *Nat. Rev. Neurosci.* **9**, 947 (2008).
4. S. A. Bunge, N. M. Dudukovic, M. E. Thomason, C. J. Vaidya, J. D. E. Gabrieli, *Neuron* **33**, 301 (2002).
5. B. L. Schlaggar *et al.*, *Science* **296**, 1476 (2002).
6. E. A. Crone, C. Wendelken, S. Donohue, L. van Leijenhorst, S. A. Bunge, *Proc. Natl. Acad. Sci. U.S.A.* **103**, 9315 (2006).
7. D. A. Fair *et al.*, *Proc. Natl. Acad. Sci. U.S.A.* **104**, 13507 (2007).
8. D. A. Fair *et al.*, *PLOS Comput. Biol.* **5**, e1000381 (2009).
9. K. Velanova, M. E. Wheeler, B. Luna, *J. Neurosci.* **29**, 12558 (2009).
10. J. V. Haxby *et al.*, *Science* **293**, 2425 (2001).
11. S. M. Polyn, V. S. Natu, J. D. Cohen, K. A. Norman, *Science* **310**, 1963 (2005).
12. K. A. Norman, S. M. Polyn, G. J. Detre, J. V. Haxby, *Trends Cogn. Sci.* **10**, 424 (2006).
13. E. Formisano, F. De Martino, M. Bonte, R. Goebel, *Science* **322**, 970 (2008).
14. F. Pereira, T. M. Mitchell, M. Botvinick, *Neuroimage* **45**, S199 (2009).
15. A. Ben-Hur *et al.*, *PLOS Comput. Biol.* **4**, e1000173 (2008).
16. Materials and methods are available as supporting material on *Science* Online.
17. J. D. Johnson, S. G. R. McDuff, M. D. Rugg, K. A. Norman, *Neuron* **63**, 697 (2009).
18. T. M. Mitchell *et al.*, *Science* **320**, 1191 (2008).
19. C. S. Soon, M. Brass, H.-J. Heinze, J.-D. Haynes, *Nat. Neurosci.* **11**, 543 (2008).
20. A. Schurger, F. Pereira, A. Treisman, J. D. Cohen, *Science* **327**, 97 (2010); published online 12 November 2009 (10.1126/science.1180029).
21. D. Zhang, M. E. Raichle, *Nat. Rev. Neurol.* **6**, 15 (2010).
22. B. B. Biswal, F. Z. Yetkin, V. M. Haughton, J. S. Hyde, *Magn. Reson. Med.* **34**, 537 (1995).
23. B. B. Biswal *et al.*, *Proc. Natl. Acad. Sci. U.S.A.* **107**, 4734 (2010).
24. C. M. Lewis, A. Baldassarre, G. Committeri, G. L. Romani, M. Corbetta, *Proc. Natl. Acad. Sci. U.S.A.* **106**, 17558 (2009).
25. H. Akaike, in *Second International Symposium on Inference Theory,* B. N. Petrov, F. Csaki, Eds. (Akademiai Kiado, Budapest, 1973), pp. 267–281.
26. A. Tsoularis, J. Wallace, *Math. Biosci.* **179**, 21 (2002).
27. K. Supekar, M. Musen, V. Menon, K. J. Friston, *PLoS Biol.* **7**, e1000157 (2009).
28. M. E. Raichle *et al.*, *Proc. Natl. Acad. Sci. U.S.A.* **98**, 676 (2001).
29. N. U. F. Dosenbach *et al.*, *Neuron* **50**, 799 (2006).
30. N. U. F. Dosenbach *et al.*, *Proc. Natl. Acad. Sci. U.S.A.* **104**, 11073 (2007).
31. P. Hagmann *et al.*, *PLoS Biol.* **6**, e159 (2008).
32. D. Tomasi, N. D. Volkow, *Proc. Natl. Acad. Sci. U.S.A.* **107**, 9885 (2010).
33. F. I. M. Craik, E. Bialystok, *Trends Cogn. Sci.* **10**, 131 (2006).
34. P. Shaw *et al.*, *J. Neurosci.* **28**, 3586 (2008).
35. L. H. Somerville, B. J. Casey, *Curr. Opin. Neurobiol.* **20**, 236 (2010).
36. P. Shaw *et al.*, *Nature* **440**, 676 (2006).
37. G. Gong *et al.*, *J. Neurosci.* **29**, 15684 (2009).
38. H. Shen, L. Wang, Y. Liu, D. Hu, *Neuroimage* **49**, 3110 (2010).

39. This work was supported by NIH grants NS55582, NS053425, HD057076, and NS00169011 (B.L.S.); NS51281, NS32979, NS41255, and NS46424 (S.E.P.); DA027046 (C.N.L.-S.); EY16336 (J.R.P.); and MH62130 (D.M.B.) and by the John Merck Scholars Fund (B.L.S.), Burroughs-Wellcome Fund (B.L.S.), Dana Foundation (B.L.S.), Ogle Family Fund (B.L.S.), McDonnell Center (S.E.P. and B.L.S.), Simons Foundation (S.E.P.), American Hearing Research Foundation (J. E. C. Lieu), and Diabetes Research Center at Washington University (T. G. Hershey). We thank J. E. C. Lieu, C. E. Pizoli, and T. G. Hershey for providing data and F. M. Miezin, J. Harwell, A. Z. Snyder, and H. M. Lugar for help with data analysis.

Supporting Online Material

www.sciencemag.org/cgi/content/full/329/5997/1358/DC1
Materials and Methods
SOM Text
Figs. S1 to S9
Tables S1 to S6
References

23 June 2010; accepted 4 August 2010
10.1126/science.1194144

ERRATUM

Post date 5 November 2010

Reports: "Prediction of individual brain maturity using fMRI" by N. U. F. Dosenbach *et al*. (10 September, p. 1358). In Fig. 2, the labels in the bottom-right image (anterior view) were incorrect. The "L" and "R" labels should be switched.

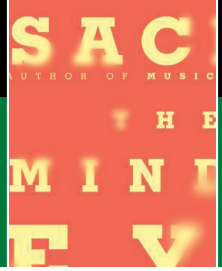

LETTERS

edited by Jennifer Sills

The Hazy Details of Early Earth's Atmosphere

IN THEIR REPORT "FRACTAL ORGANIC HAZES PROVIDED AN ULTRAVIOLET SHIELD FOR EARLY Earth" (4 June, p. 1266), E. T. Wolf and O. B. Toon base their fractal haze theory on the assumption that the Archean atmosphere was primarily N_2. The Report includes no reference for this "prevailing view," and much evidence can be amassed against it. Geologists since Darwin have uniformly argued for a CO_2-dominant atmosphere for the early Earth (*1*, *2*).

The evolutionary roots of biochemistry draw on CO_2 and H_2 as the main nutrients of life. Life also requires the extra proton power afforded by chemiosmosis, an energy source that must have been available to emergent life (*3*–*5*). Primordial metabolism may have been based on minerals catalyzing the reaction between CO_2 and H_2 via the acetyl coenzyme-A pathway (*6*). Furthermore, data that enzymes involved in synthesizing sugars predate those that catabolize them (*7*) does not support the theory that catabolism of preformed organic molecules was the driver to life's emergence.

C. F. Chyba ("Countering the early faint Sun," Perspectives, 4 June, p. 1238) offers one alternative (i.e., autogenic) model: Wächtershäuser's surface metabolism (*8*). However, this hypothesis fails because the initial conditions invoked offer neither a natural protonmotive force to drive biosynthesis, nor a compartment for its focus. The alkaline hydrothermal hypothesis does address this (*8*) and other aspects of life's onset, in a model that leads logically to the acetyl coenzyme-A pathway, without resorting to contingency (*9*).

MICHAEL JOHN RUSSELL

Planetary Science, Jet Propulsion Laboratory, Pasadena, CA 91109–8099, USA. E-mail: mrussell@jpl.nasa.gov

References

1. B. J. Wood *et al.*, *Science* **248**, 337 (1990).
2. H. Ohmoto *et al.*, *Nature* **429**, 395 (2004).
3. M. J. Russell *et al.*, *Terra Nova* **5**, 343 (1993).
4. W. Martin, M. J. Russell, *Philos. Trans. R. Soc. London Ser. B* **362**, 1887 (2007).
5. W. Nitschke, M. J. Russell, *J. Mol. Evol.* **69**, 481 (2009).
6. I. A. Berg *et al.*, *Nat. Rev. Microbiol.* **8**, 447 (2010).
7. R. F. Say, G. Fuchs, *Nature* **464**, 1077 (2010).
8. G. Wächtershäuser, *Microbiol. Rev.* **52**, 452 (1988).
9. M. J. Russell, W. Martin, *Trends Biochem. Sci.* **29**, 358 (2004).

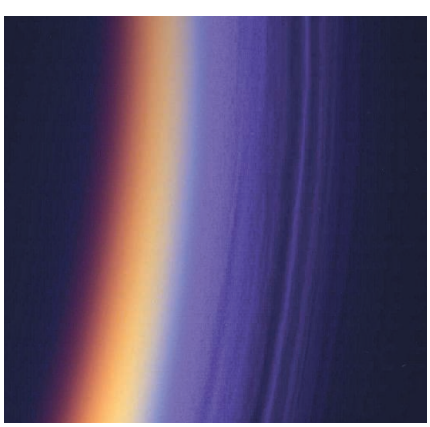

Titan's haze. Early Earth's atmosphere may have resembled that of Saturn's moon Titan.

CREDIT: JPL/NASA

Response

RUSSELL ARGUES THAT A TITAN-LIKE VIEW of the early Earth is inaccurate and that a CO_2-dominated atmosphere is more likely. This view dominated thinking in the 1980s and 1990s, but has since been in decline. Geochemical arguments have been made supporting low CO_2 abundances. Rosing *et al.* argue that the presence of magnetite in banded-iron formations constrains atmospheric CO_2 to a mere 3 times the present atmospheric level (*1*). Moreover, vigorous plate tectonics would likely have sequestered most CO_2 within the mantle (*2*). Russell assumes that N_2 was not likely the dominant gas. However, Goldblatt *et al.* (*3*) suggest that a higher fraction of Earth's total nitrogen budget was present in the young atmosphere than today. In contrast to Russell's assumptions, these recent studies point toward a young atmosphere dominated by N_2 and requiring greenhouse gases in addition to CO_2 to keep the young Earth warm.

Admittedly, achieving high methane concentrations before organic material existed on Earth is difficult (*4*). However, methane concentrations of 1000 parts per million or higher supplied by methanogens are predicted for the postbiotic Earth (*5*). When the CH_4/CO_2 ratio rose above 0.1, N_2–CH_4 photochemistry could proceed (*6*), creating the ultraviolet-shielding fractal organic haze we described. Ammonia could have been protected from photolysis beneath the haze, yielding an atmosphere rich in both CH_4 and NH_3, thus making it possible for these inorganic material to yield organic compounds (Miller-Urey chemistry), as we noted in our Report.

Although our work makes no attempt to address the specific biochemical mechanisms that lie at roots of life, we do address important questions regarding the atmospheric composition and climate of the Earth at the time when life first flourished. Recent studies (*6*, *7*) along with the evidence amassed against a CO_2-rich atmosphere indicate that the Archean was at least mildly reducing. Whether the very first life was formed as a direct result of chemical reactions of inorganic material, as indicated by Miller-Urey chemistry, is up for debate, but given the emerging new picture of the Archean, surely Miller-Urey chemistry would have proceeded at some point early in the Earth's history. The haze chemistry itself would have produced organics at a rate that would likely dwarf the production of organics from the hydrothermal vent systems favored by Russell (*5*). Laboratory studies have confirmed that complex organics are readily produced in early Earth–like environments

Published by AAAS

containing N_2, CO_2, CH_4, and H_2 (*8*). The organic haze particles may have been edible and would have precipitated into the young oceans, creating an organic soup consistent with Miller-Urey (*9*).

E. T. WOLF* AND O. B. TOON

Laboratory for Atmospheric and Space Physics, Department of Atmospheric and Oceanic Sciences, University of Colorado, Boulder, CO 80309–0392, USA.

*To whom correspondence should be addressed. E-mail: eric.wolf@colorado.edu

References

1. M. T. Rosing, D. K. Bird, N. H. Sleep, C. J. Bjerrum, *Nature* **464**, 744 (2010).
2. N. H. Sleep, K. Zahnle, *J. Geophys. Res.* **106**, 1373 (2001).
3. C. Goldblatt *et al*., *Nat. Geosci.* **2**, 891 (2009).
4. J. F. Kasting, *Precambrian Res.* **137** 119 (2005).
5. A. A. Pavlov, L. L. Brown, J. F. Kasting, *J. Geophys. Res.* **106** 23267 (2001).
6. J. D. Haqq-Misra, S. D. Domagal-Goldman, P. J. Kasting, J. F. Kasting, *Astrobiology* **8** 1127 (2008).
7. F. Tian, O. B. Toon, A. A. Pavlov, H. De Sterck, *Science* **308** 1014 (2005).
8. H. L. Dewitt *et al.*, *Astrobiology* **9** 447 (2009).
9. M. G. Trainer *et al.*, *Astrobiology* **4** 409 (2004).

Response

RUSSELL PROPOSES THAT EARLY EARTH'S atmosphere contained primarily CO_2 and lacked N_2. For this idea to make sense, one must explain how volcanic outgassing or comet/asteroid impact delivery of the early atmosphere's constituents could provide CO_2 yet sequester N_2.

In my Perspective, I focused on the implications of the Wolf and Toon Report for early Earth's greenhouse; I only briefly touched on its implications for the origin of life. Wolf and Toon's model removes one of the long-standing objections to an early atmosphere with substantial methane and ammonia, and therefore to the Miller-Urey organic "building block" approach to the origin of life. Their model cannot speak to other important objections to the building-block hypothesis. I contrasted the Miller-Urey picture with metabolism-first theories in which life originates with autocatalytic cycles (cycles in which the product of the chemical reaction is also a reactant) that use inorganic carbon such as CO_2 (*1*). Clearly, metabolism-first theories are now a burgeoning subfield of their own (*2*). More recent discoveries of hydrothermal venting far from ocean ridges (*3*) have propelled alkaline-environment metabolism-first theories, such as the one Russell describes, into the spotlight (*4*).

Huber and Wächtershäuser (*5*) showed that the crucial reaction in the acetyl coenzyme-A pathway that Russell favors could have occurred prebiotically (before life existed), supporting the idea that metabolism

Published by AAAS

could have evolved from prebiotic chemistry. A centrality of the acetyl coenzyme-A path to the origin of life is therefore broadly consistent with the Wächtershäuser approach, although there are important differences, which Russell argues favors his model (*6*). The alkaline model for life's origin may also be relevant to Jupiter's moon Europa (*7*).

Complex environmental questions about early Earth and the origin of life may well have composite answers. Researchers need to understand the strengths, weaknesses, and possible complementary roles of multiple approaches to the problem.

CHRISTOPHER F. CHYBA

Department of Astrophysical Sciences, Princeton University, Princeton, NJ 08544, USA. E-mail: cchyba@princeton.edu

References

1. G. Wächtershäuser, *Microbiol. Rev.* **52**, 452 (1988).
2. G. D. Cody, J. H. Scott, in *Planets and Life*, W. T. Sullivan, J. A. Baross, Eds. (Cambridge Univ. Press, Cambridge, 2007), pp. 174–186.
3. D. S. Kelley *et al.*, *Nature* **412**, 145 (2001).
4. W. Martin, J. Baross, D. Kelley, M. J. Russell, *Nature Rev. Microbiol.* **6**, 806 (2008).
5. C. Huber, G. Wächtershäuser, *Science* **276**, 245 (1997).
6. M. J. Russell, *Science* **302**, 580 (2003).
7. K. P. Hand, C. F. Chyba, J. C. Priscu, R. W. Carlson, K. H. Nealson, in *Europa*, R. T. Pappalardo, W. B. McKinnon, K. Khurana, Eds. (Univ. of Arizona Press, Tucson, AZ, 2009), pp. 589–629.

Funding for Chinese Collaboration

IN THEIR EDITORIAL "CHINA'S RESEARCH CULTURE" (3 September, p. 1128), Y. Shi and Y. Rao describe an example of the rampant problems in China's research funding allocation, namely the selection of recipients for "mega-project grants." I often hear stories about very expensive equipment left packed in hallways or labs for years without being used. The funding agencies often have very strict guidelines for using the funding on salaries, even though a research group's ability to hire the talent they need is often the most important factor in the success of the research program.

China's funding strategy for overseas Chinese scientists is also problematic. As part of an Asia-wide trend, China has been trying to recruit talents from overseas (*1*). To attract established overseas Chinese researchers with advanced education from western countries, China has devoted billions of Chinese yuan to talent programs [such as the Thousand Talent program (*2*) recently established by the central government] that require overseas scholars to relocate to China to accept prestigious full-time positions. However, many recipients of these awards cannot relocate because of practical and family obligations.

China should focus instead on grants that fund collaborative research between overseas Chinese scholars and their peers in China. Collaborative programs are more cost-effective and more practical for those who cannot relocate. One such program is the Joint Research Fund (JRF) for Overseas Chinese Scholars and Scholars in Hong Kong and Macao, administered by the National Natural Science Foundation of China (NSFC). In 2006, a mere 0.7% of the NSFC budget was allocated to this worthy program (*3*). In 2008, the maximum grant was reduced from 400,000 Chinese yuan over 3 years to 200,000 Chinese yuan over 2 years (*4*, *5*). By dedicating such a small budget to this program and others like it, China misses an opportunity to engage overseas Chinese scholars and benefit from their contributions to the country's research and education.

SCOTT X. CHANG

Department of Renewable Resources, University of Alberta, Edmonton, AB T6G 2E3, Canada. E-mail: scott.chang@ualberta.ca

References

1. A. S. Huang, C. Y. H. Tan, *Science* **329**, 1471 (2010).
2. Thousand Talent program [www.1000plan.org (in Chinese)].
3. National Natural Science Foundation of China, Financial Statistics of NSFC in 2006 (www.nsfc.gov.cn/english/11st/index.html).
4. National Natural Science Foundation of China, Fund for Talented Professionals (NSFC, 2008), p. 17; www.nsfc.gov.cn/english/06gp/pdf/2008/051.doc.
5. National Natural Science Foundation of China, Funds for Talented Professionals (NSFC, 2007), p. 145; www.nsfc.gov.cn/english/06gp/pdf/2007/031.pdf.

CORRECTIONS AND CLARIFICATIONS

Brevia: "Pulsar discovery by global volunteer computing" by B. Knispel *et al.* (10 September, p. 1305). The Einstein@Home data are transferred to the Albert Einstein Institute (not Liebniz Universität) in Hannover, Germany.

Reports: "Prediction of individual brain maturity using fMRI" by N. U. F. Dosenbach *et al.* (10 September, p. 1358). In Fig. 2, the labels in the bottom-right image (anterior view) were incorrect. The "L" and "R" labels should be switched.

Reports: "Unprecedented restoration of a native oyster metapopulation" by D. M. Schulte *et al.* (28 August 2009, p. 1124). Reference 19 was incorrect. The correct reference is "K. Greenhawk, T. O'Connell, L. Barker, Oyster Population Estimates for the Maryland Portion of Chesapeake Bay 1994–2006 (Maryland Department of Natural Resources, 2007), Table 7; www.dnr.state.md.us/fisheries/oysters/mtgs/MDOysterPopEst_07_27_07.pdf."

Letters to the Editor

Letters (~300 words) discuss material published in *Science* in the previous 3 months or issues of general interest. They can be submitted through the Web (www.submit2science.org) or by regular mail (1200 New York Ave., NW, Washington, DC 20005, USA). Letters are not acknowledged upon receipt, nor are authors generally consulted before publication. Whether published in full or in part, letters are subject to editing for clarity and space.

Published by AAAS